tain two zooxanthella RFLPs: the group C RFLP plus a unique RFLP generated by one nucleotide substitution that creates a Taq I site in the larger of the two RFLP C fragments (*14*). These two RFLPs either represent two distinct algae or a polymorphism within the multicopy ssRNA genes of one alga. Some other digests contain extra fragments that may identify additional ssRNA sequences. These represent small PCR amplification products that cannot be complete ssRNA genes (for example, Fig. 1C, lanes 1 and 6), or they are not interpretable from the available data; where those products occur, they occur in all individuals of that host species.
16. Replicates (Table 1) were collected from different locations so that distinct individuals, as opposed to members of one or a few clones, were sampled.
17. C. Yanisch-Perron, J. Vieira, J. Messing, *Gene* **33**, 103 (1985).
18. In phylogenetic analyses, sequences determined from cloned PCR-amplified ssRNA genes include an uncertainty owing to the possibility of DNA replication errors during PCR, and of sequence polymorphism within multicopy ssRNA genes [M. L. Sogin, in *PCR Protocols: A Guide to Methods and Applications*, M. A. Innis, D. H. Gelfand, J. J. Sninsky, T. J. White, Eds. (Academic Press, New York, 1990), pp. 307–314]. Replicate sequencing suggests that this uncertainty is on the order of one or two nucleotides for the ssRNA region that we studied (*13*).
19. M. J. Kevin, W. T. Hall, J. J. A. McLaughlin, P. A. Zahl, *J. Phycol.* **5**, 341 (1969).
20. M. L. Sogin, A. Ingold, M. Karlok, H. Nielsen, J. Engberg, *EMBO J.* **5**, 3625 (1986).
21. T. W. Vaughan and J. W. Wells, *Spec. Papers Geol. Soc. Am. 44* (1943).
22. The validity of using RFLP genotypes to classify these zooxanthellae is explicitly demonstrated by their concordance with the phylogenetic groups defined by ssRNA sequences (Fig. 3).
23. A. G. Coates and J. B. C. Jackson, *Paleobiology* **13**, 363 (1987); G. D. Stanley, Jr., *Geology* **9**, 507 (1981).
24. I. Leizerovich, N. Kardish, M. Galun, *Symbiosis* **8**, 75 (1990).
25. T. F. Goreau, *Science* **145**, 383 (1964); P. W. Glynn, *Environ. Conserv.* **10**, 149 (1983).
26. J. Maynard Smith, *The Evolution of Sex* (Cambridge Univ. Press, Cambridge, MA, 1978).
27. L. W. Buss, *The Evolution of Individuality* (Princeton Univ. Press, Princeton, NJ 1987).
28. T. H. Jukes and C. R. Cantor, in *Mammalian Protein Metabolism*, H. N. Munro, Ed. (Academic Press, New York, 1969), pp. 21–132.
29. J. Felsenstein, PHYLIP Version 3.2 Manual (University of California Herbarium, Berkeley, CA, 1989).
30. R.R. thanks L. Brezinsky, C. Kanechika, and T. Humphrys for hospitality and laboratory space on Oahu, and colleagues at the West Indies Laboratory and the National Undersea Research Center on St. Croix for their help in collecting specimens. M. A. Coffroth supplied *Plexaura* A samples. L. Park and C. Patton got the PHYLIP programs running. Supported by an NSF Postdoctoral Fellowship in Marine Biotechnology (R.R.) and by a contract from the National Undersea Research Center, National Oceanic and Atmospheric Administration.

17 August 1990; accepted 19 December 1990

Recombinase-Mediated Gene Activation and Site-Specific Integration in Mammalian Cells

STEPHEN O'GORMAN,* DANIEL T. FOX, GEOFFREY M. WAHL

A binary system for gene activation and site-specific integration, based on the conditional recombination of transfected sequences mediated by the FLP recombinase from yeast, was implemented in mammalian cells. In several cell lines, FLP rapidly and precisely recombined copies of its specific target sequence to activate an otherwise silent β-galactosidase reporter gene. Clones of marked cells were generated by excisional recombination within a chromosomally integrated copy of the silent reporter. By the reverse reaction, integration of transfected DNA was targeted to a specific chromosomal site. The results suggest that FLP could be used to mosaically activate or inactivate transgenes for analysis of vertebrate development, and to efficiently integrate transfected DNA at predetermined chromosomal locations.

RECENT ANALYSES OF MAMMALIAN development have made use of transfected genes to alter cell interactions and trace cell lineages. This inherently powerful approach could be applied to investigate a broader range of developmental processes if it was possible to restrict transgene expression to specific subsets of the cells, tissues, or developmental stages in which the cis-acting sequences that typically control expression are active. Such mosaic expression is essential for many forms of lineage analyses and would additionally provide a means to assess the effects of transgenes that grossly alter development in small patches of tissue within an otherwise normal embryo. Toward this end, we have characterized a conditional recombination system based on the site-specific recombinase, termed FLP (*1*), from *Saccharomyces cerevisiae*. In this system, gene activation requires prior FLP-mediated excisional recombination, and expression therefore falls under the binary control of the transgene's own cis-acting sequences and those that direct FLP expression. Reversal of this excisional recombination, under different experimental conditions, provides a means for introducing DNA into specific sites in mammalian chromosomes.

Gene Expression Laboratory, The Salk Institute for Biological Studies, La Jolla, CA 92037.

*To whom correspondence should be addressed.

A cotransfection assay was used to characterize FLP-mediated recombination of extrachromosomal DNA in a variety of cell lines. Cells were transfected with an expression construct and a "reporter" plasmid that was a substrate for the recombinase. The activity of the expression construct was assayed either by recovering the transfected reporter and looking for molecular evidence of recombination or by preparing cytoplasmic extracts to measure β-galactosidase activity generated by precisely recombined reporter molecules.

The pNEOβGAL reporter plasmid used in these assays was derived from pFRTβGAL (Fig. 1A). pFRTβGAL contains the bacterial β-galactosidase coding sequence, which has been modified by insertion of an FLP recombination target site (FRT) immediately 3′ to the translational start (*2*). The FRT consisted of the two inverted 13–base pair (bp) repeats and 8-bp spacer that comprise the minimal FLP target (*3, 4*) plus an additional 13-bp repeat that may augment reactivity of the minimal sub-

Table 1. β-Galactosidase activities in cotransfection assays of 293, CV-1, and F9 cells. Positive control transfections (pFRTβGAL) included 1 μg of pFRTβGAL and 18 μg of the pOG28 (*6*) non-FLP control plasmid. Negative control transfections (pNEOβGAL) included 1 μg of pNEOβGAL and 18 μg of pOG28. Experimental transfections (pNEOβGAL + FLP) contained 1 μg of pNEOβGAL and 18 μg of the pOG44 FLP expression plasmid (Fig. 1A). The pNEOβGAL + FLP values are also shown as a percentage of the pFRTβGAL positive control values. Each value represents the mean and SEM of six plates from two experiments. Neither pOG28 nor pOG44 generated β-galactosidase activity when transfected alone (*5*). Transfections and assays were performed as described in the legend to Fig. 1. All transfections contained 1 μg of pRSVL to correct β-galactosidase activities for relative transfection efficiencies.

Cell line	β-Galactosidase activity (units/mg protein)			
	pFRTβGAL	pNEOβGAL	pNEOβGAL + FLP	$\frac{\text{pNEOβGAL + FLP}}{\text{pFRTβGAL}}$ (%)
293	30.4 ± 1.9	0.17 ± 0.02	14.2 ± 2.2	47
CV-1	275 ± 25	0.33 ± 0.06	22.6 ± 1.2	8
F9	24.8 ± 4.3	0.04 ± 0.01	1.88 ± 0.02	8

strate (*4*). The insertion preserved the β-galactosidase translational reading frame and pFRTβGAL generated robust activity in mammalian cells (Table 1). pNEOβGAL was constructed by cutting pFRTβGAL within the FRT with Xba I and then inserting an Xba I fragment that consisted of two half-FRT sites flanking a neomycin transcription unit (*2*). This created intact FRTs on each side of the neomycin cassette and rendered the β-galactosidase transcription unit inactive (Table 1). Because the two FRT sites in pNEOβGAL are tandemly arrayed, precise FLP-mediated recombination of the FRTs would be expected to excise the neomycin cassette, re-create the parental pFRTβGAL plasmid, and restore β-galactosidase expression.

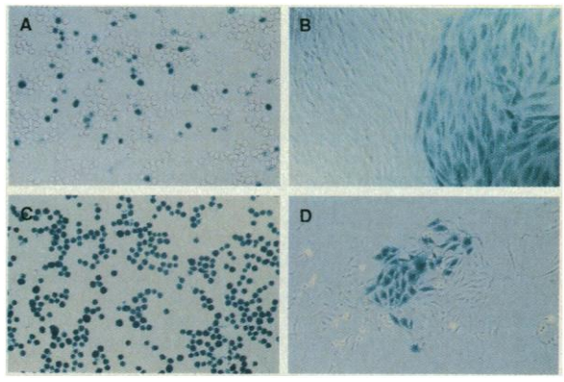

Fig. 2. Histochemical demonstration of β-galactosidase activity in cell lines with a single integrated copy of pNEOβGAL after transfection with the pOG44 FLP expression plasmid. (**A**) CVNEOβGAL/E26 cells 48 hours after transfection. Cells that express β-galactosidase contain a blue reaction product. (**B**) Border between positive and negative colonies of CVNEOβGAL/E25 cells 2 weeks after transfection. (**C**) The B2 subclone of CVNEOβGAL/E25 after 8 weeks of culture. (**D**) A mixed colony of CVNEOβGAL/E25 cells 1 week after transfection showingboth positive and negative cells. CVNEOβGAL/E cells growing under G418 selection were transferred to nonselective medium and transfected 24 hours later with pOG44 as described in the legend to Fig. 1. Cells were histochemically processed (*26*) either with (A and D) or without (B and C) prior resuspension.

Cotransfection of cells with a fixed amount of pNEOβGAL and increasing amounts of an FLP expression vector (pOG44) generated increasing amounts of recombined reporter plasmid and β-galactosidase activity. Molecular evidence for FLP-mediated recombination was obtained by recovering plasmids 36 hours after transfection, followed by restriction endonuclease treatment and Southern (DNA) blotting (Fig. 1B). Lysates of cells from cotransfections that included pOG44 showed a signal at 5.6 kb, which corresponds to the size of recombined reporter (equivalent to pFRTβGAL), and a 3.2-kb signal that was generated by unrecombined pNEOβGAL receptor (Fig. 1A). The 5.6-kb band intensity was proportional to the amount of FLP expression plasmid included in the transfection, and this band was not seen in cotransfections in which a non-FLP plasmid was substituted for the FLP expression vector (Fig. 1B) or in transfections that only contained pOG44 (*5*). The pOG44 vector generated additional signals at 2.2 and 2.8 kb because it contained sequences homologous to the probe (*6*). In the same samples, β-galactosidase activity was also proportional to the amount of FLP expression plasmid included (Fig. 1C). Only background activities were observed in cotransfections that included a non-FLP control plasmid (Table 1) or when pOG44 alone was transfected (*5*). The experiment thus provides both molecular and biochemical evidence for precise FLP-mediated recombination.

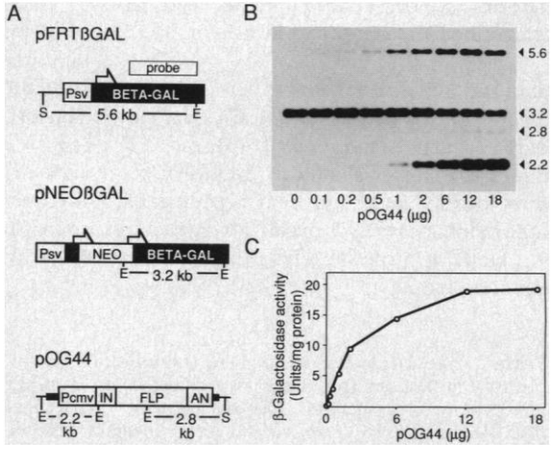

Fig. 1. Cotransfection assay for FLP-mediated recombination of extrachromosomal DNA. (**A**) pFRTβGAL, pNEOβGAL, and the pOG44 FLP expression vector (*6*). Half-arrows, positions of FRT sites; E and S, Eco RI and Sca I restriction sites; respectively; Psv, early promoter from SV40; BETA-GAL, β-galactosidase coding sequence; NEO, neomycin expression cassette; Pcmv, cytomegalovirus immediate-early promoter; IN, intron; FLP, FLP coding sequence; AN, SV40 adenylation cassette. Thin lines represent vector sequences; thick lines in the pOG44 diagram represent sequences homologous to the probe. Sizes of restriction fragments are indicatedin kilobase pairs (kb). (**B**) Southern blot of Hirt lysates (*21*) prepared from 293 (human embryonic kidney) (*22*) cells transfected with 1 μg of pNEOβGAL and varying amounts of pOG44. A non-FLP control plasmid (pOG28) (*6*) was included as needed to keep the total amount of plasmid and Pcmv constant. Sizes of fragments (kilobase pairs) are shown at right. Lysates were digested with Eco RI and Sca I, and Southern blots were probed with a β-galactosidase probe (Fig. 1A). The identities of the hybridizing bands were confirmed with additional digests and probes. (**C**) β-Galactosidase activities in the same transfections shown in (B). Subconfluent cultures of cells growing in Dulbecco's minimum essential medium and 5% calf serum in 10-cm dishes were transfected by overnight exposure to calcium phosphate precipitates (*23*) and then divided into four lots. After 24 hours of incubation, one plate of each transfection was harvested by Hirt extraction (*21*), and a second plate was used to prepare cytoplasmic extracts (*24*). Approximately 5% of the DNA recovered from single plates was used for Southern analyses. β-Galactosidase assays were performed as described (*25*). Luciferase activities generated by the inclusion of 1 μg of pRSVL (*24*) in all transfections were used to correct β-galactosidase activities for relative transfection efficiencies. The experiment was repeated twice with similar results.

This paradigm was used to demonstrate FLP activity in monkey kidney (CV-1) and mouse embryonal carcinoma (F9) cells. In Table 1, the β-galactosidase activities in the "pFRTβGAL" transfections represent an estimate of the expression expected if all the pNEOβGAL in a cotransfection immediately underwent recombination. The highest relative expression in pNEOβGAL plus pOG44 cotransfections, 47%, occurred in 293 cells; this is a high level of activity considering that β-galactosidase expression required prior FLP expression and recombination of pNEOβGAL. Cotransfections of CV-1 and F9 cells generated 8% of the activity seen in the pFRTβGAL transfections. Even this lower relative activity clearly marked cotransfected cells in histochemical reactions for β-galactosidase activity (*5*).

For this method of gene activation to be useful in transgenic mice, FLP would need to routinely mediate recombination of FRTs integrated at a single site in the mammalian genome. Cell lines that contained single integrated copies of pNEOβGAL (designated CVNEOβGAL/E) were isolated by transfecting CV-1 cells with linearized plasmids by electroporation, selecting G418-resistant ($G418^R$) transfectants that stably expressed the neomycin cassette, and identifying single copy lines by Southern blot analyses (*5*) (Fig. 3). As previously shown for other integrated constructs with similarly short direct repeats (*7*), the chromosomal FRTs did not spontaneously recombine to produce a β-galactosidase–positive (βGAL^+) phenotype at detectable frequencies (Table 2).

Transient expression of FLP in the CVNEOβGAL/E lines promoted a rapid conversion to a βGAL^+ phenotype. When five different cell lines were transfected with pOG44, β-galactosidase activities after 36

Table 2. β-Galactosidase phenotypes of CVNEOβGAL/E cell lines (which contain a single inactive copy of the pNEOβGAL reporter) after transfection with FLP expression (pOG44), non-FLP negative control (pOG28), or β-galactosidase positive control (pFRTβGAL) plasmids. The pFRTβGAL transfections included 1 μg of pFRTβGAL and 19 μg of pOG44; other mixes contained 20 μg of the indicated plasmid. β-Galactosidase activities are mean values for triplicate transfections performed as described in the legend to Fig. 1 and assayed 36 hours after removal of precipitates; SEM values for the pOG44 transfections were less than 10% of the means. The β-galactosidase phenotype of cells was determined by scoring more than 10^3 cells after transfection and histochemical processing as described in the legend to Fig. 2.

Cell line	β-Galactosidase activity (units/mg protein)		βGal$^+$ cells (%)		
	pOG28	pOG44	pOG28	pFRTβGAL	pOG44
E6	0.24	11.2	0*	8.7	6.1
E25	0.21	16.7	0*	17.1	12.4
E26	0.18	7.2	0*	19.5	15.4
E14	0.28	13.1	ND	ND	ND
E22	0.09	9.6	ND	ND	ND

*No positive cells were detected among $>10^6$ cells examined. ND, not determined.

hours were 40 to 100 times as high as those seen in replicate plates transfected with a non-FLP plasmid (Table 2). At 48 hours after transfection, histochemical processing showed many βGAL$^+$ cells (Table 2 and Fig. 2A). To provide some estimate of the efficiency of recombination, we prepared an additional set of replicate plates that were transfected with pFRTβGAL. A comparison of the fractions of βGAL$^+$ cells in the pFRTβGAL and in the pOG44 transfections suggests, assuming similar transfection efficiencies, that most of the cells (70 to 80%) transfected with pOG44 were converted to a βGAL$^+$ phenotype (Table 2). The comparison undoubtedly underestimates the efficiency of FLP-mediated excision because many copies of a functional β-galactosidase gene were available for immediate transcription in the positive controls, whereas recombination may have occurred only shortly before harvest in some pOG44-transfected cells; in these cases, the single recombined reporter gene may not have generated enough β-galactosidase by the time of harvest to render the cells positive in the assay.

The βGAL$^+$ phenotype was passed on to all descendents of many FLP-converted cells. Positive colonies were formed when transfected cells were plated at low densities (Fig. 2B), and β-galactosidase expression persisted during prolonged expansion of individual colonies (Fig. 2C). Entirely negative colonies (Fig. 2B) and mixed colonies (Fig. 2D) were also observed. Mixed colonies would be expected if recombination occurred after mitosis in only one descendant of a transfected cell, or if recombined and unrecombined cells mixed at replating or during subsequent growth. Indeed, the physical segregation of phenotypes evident in most mixed colonies suggested that they were composed of stably positive and negative lineages (Fig. 2D).

The correlation between β-galactosidase expression and recombination at FRT sites was examined by comparing the structure of the integrated pNEOβGAL sequences in two βGAL$^+$ subclones to the parental line. CVNEOβGAL/E25 (E25) cells (10^6) were transfected with pOG44 and subcloned 12 hours after removal of the precipitate. After histochemical screening, two βGAL$^+$ subclones (E25B1 and E25B2) were expanded for further analysis. In Southern blots of genomic DNA from both subclones, the pattern of hybridization matched that expected for FLP-mediated recombination of the FRT sites in the parental line (Fig. 3). In Eco RI digests, the 3.2-kb fragment of E25 was lost and 2.0 kb of DNA were added to an 8.5-kb junctional fragment to create a 10.5-kb junctional fragment in the derived lines. The other (3.7-kb) junctional fragment and the internal 2.0-kb fragment were unchanged. Although recombination products have not been recovered and sequenced, these Southern analyses and the fact that activation of β-galactosidase expression required creation of functional translational reading frame suggest that the preponderance of FLP-mediated recombination was precise.

Reversal of this excisional recombination could in principle be used to target the integration of transfected plasmids containing an FRT to specific genomic sites. To compare the frequency of such site-specific integration to the frequency of integration at random sites, we cotransfected G418-sensitive, βGAL$^+$ E25B2 cells with pOG44 and a plasmid, pOG45, that contained a neomycin resistance gene expression cassette and a single FRT (*8*). We expected that G418^R colonies formed after site-specific integration of pOG45 would be β-galactosidase–negative (βGAL$^-$), whereas those formed by random integration would be βGAL$^+$. G418^R subclones (designated B2N) were histochemically stained and more than half were found to be either entirely βGAL$^-$, or predominantly βGAL$^-$ with a few clusters of βGAL$^+$ cells (Table 3). The remaining colonies were βGAL$^+$. With continued passage as dispersed monolayers, the fraction of βGAL$^+$ cells in the mixed lines rapidly diminished. The possibility that they were G418-sensitive cells that initially survived because of their proximity to resistant cells was confirmed by reconstitution experiments (*5*). All of the colonies formed after parallel cotransfections of pOG44 and control plasmids containing the same neomycin cassette but lacking an FRT were βGAL$^+$ (Table 3).

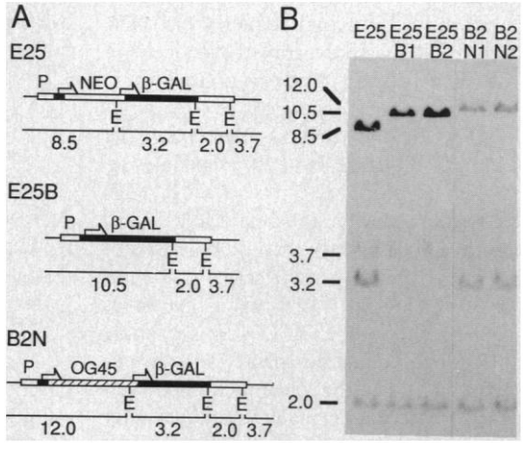

Fig. 3. Analysis of genomic DNA from a cell line with a single integrated copy of pNEOβGAL (CVNEOβGAL/E25 or E25), two derivative βGAL$^+$ subclones (E25B1, E25B2), and two subclones derived from E25B2 after cotransfection with pOG45 and pOG44 (B2N1, B2N2). (**A**) Top, pattern of plasmid integration in E25 deduced from Southern blot analysis; middle, predicted pattern for βGAL$^-$ subclones of E25 if precise recombination across the FRTs occurred; bottom, predicted pattern for βGAL$^+$ G418^R subclones of E25B2 after FLP-mediated insertion of pOG45. Abbreviations and symbols as in Fig. 1A; except here P denotes the SV40 early promoter; β-GAL, β-galactosidose coding sequence; thin lines represent genomic DNA; and pOG45 sequences are indicated by cross-hatching. The sizes of hybridizing fragments are given in kilobase pairs. (**B**) Southern blot of Eco RI–digested genomic DNA from the E25 parental line, the E25B1 and E25B2 subclones, and the B2N1 and B2N2 subclones of E25B2. The sizes of hybridizing fragments (kilobase pairs) are indicated at the left. The pattern predicted for precise FLP-mediated recombination was observed in all derived subclones (Fig. 3A). The probe was random-primed pNEOβGAL (Fig. 1A). The identities of the bands were confirmed with additional digests and probes.

The fidelity with which loss of β-galactosidase activity was caused by the expected recombination of chromosomal and plasmid FRTs, resulting in the integration of a single unrearranged copy of pOG45 within the β-galactosidase sequence of the E25B2 line, was examined by Southern analyses. Because the FRT and neomycin cassette of pOG45 were derived from the neomycin cassette and 3′ FRT of pNEOβGAL (Fig. 1A) (*8*), recombination of the plasmid FRT with the E25B2 chromosomal FRT would be expected to regenerate the 3.2-kb Eco RI fragment of the original E25 parent. Additionally, the 8.5-kb junctional fragment of E25 would be expected to shift to 12.0 kb because pOG45 is 3.5 kb larger than the neomycin cassette of pNEOβGAL. Finally, the 3.7-kb junctional fragment and the 2.0-kb internal fragment of the E25 and E25B lines would be expected to be unchanged in the B2N lines. These predictions were met in each of the eight βGAL^- or mosaic B2N lines analyzed, as shown for two lines in Fig. 3B. In contrast, each of the four βGAL^+ colonies examined by Southern analyses had integrated pOG45 at a random genomic site (*5*).

Our data show that FLP-mediated recombination can target the integration of transfected DNA to a specific chromosomal site at frequencies that exceed those of random integration, and that the event can be marked by an alteration in gene activity at the target site. The efficiency of targeted integration could potentially be increased by using ratios of the integrating and FLP expression vectors different from those used here, or by using FRT mutations in the plasmid and chromosomal sites to decrease the frequency at which successfully integrated plasmids are subsequently excised (*9*). The β-galactosidase–marking paradigm could be combined with a promoter-trap strategy, similar to that used to demonstrate site-specific integration mediated by the Cre recombinase (*10*). This would greatly increase the relative frequency of site-specific events.

Previous descriptions of recombinase-mediated rearrangement of chromosomal sequences in *Drosophila* (*11*) and mammalian cells (*12*) have not directly addressed the question of whether site-specific recombinases could routinely create a functional translational reading frame, as we have now shown. Moreover, the efficiency of this FLP-based system appears to be much higher than that reported in the only other description of site-specific recombination of chromosomal sequences in mammalian cells (*12*). Transient expression of the Cre recombinase in mouse L cells was shown to effect a 25-fold increase in the incidence of a selectable phenotype that required rearrangement of chromosomally integrated Cre targets. The much greater signal-to-noise ratio seen in our FLP system ($>10^6$) is in part due to the low rate at which integrated copies of pFRTβGAL spontaneously recombine, and may additionally reflect differences inherent to the recombinases or differences in the vectors used for their expression. Construction of pOG44 was guided by reports that transcript splicing can enhance or diminish expression. An intron was inserted within the untranslated leader to increase expression (*13*) and care was taken to eliminate cryptic splice acceptor sites (*14*) that are found immediately 3′ to the native FLP structural sequence (*15*). The latter could inactivate transcripts by inappropriately splicing to cryptic donor sites in the FLP structural sequence (*16*).

Earlier FLP constructs containing the structural sequence and 3′ flanking sequences in pSV2 (*17*) or pCDM8 (*18*) vectors were inactive in some cell lines and considerably less active than pOG44 in others (*5*). Surprisingly, their activity, but not that of pOG44, increased two to five times after heat shock at 45°C (*5*). As a possible explanation for this augmented expression, we propose that the accumulation of unspliced transcripts in mammalian cells after heat shock (*19*) would transiently decrease inappropriate splicing and increase the number of functional FLP transcripts, an effect that may have contributed to the robust heat shock–induced expression of FLP seen in *Drosophila* (*11, 20*).

Table 3. Numbers of $G418^R$ colonies with βGAL^+ and βGAL^- phenotypes formed after transfection of E25B2 cells with plasmids that contained a neomycin resistance gene and that additionally either did (+FRT) or did not (−FRT) contain an FRT. All transfections also included an FLP expression vector. Colonies were scored as βGAL^- if they were completely or predominantly βGAL^-, βGAL^+ colonies were always entirely positive. In one experiment (Exp 1), 10^6 cells were transfected by electroporation in 0.8 ml of phosphate-buffered saline containing 39 μg of pOG44 and 1 μg of either pOG45 (+FRT) or pMC1neo (*27*) (−FRT). In a second experiment (Exp 2), 10^6 cells were transfected by overnight exposure to calcium phosphate precipitates containing 19 μg of pOG44 and 1 μg of either pOG45 (+FRT) or pOG45A (*8*) (−FRT) as described in the legend to Fig. 1. Colonies were scored by histochemical assay (*26*) after 14 to 18 days of growth in the presence of G418.

	Number of $G418^R$ colonies			
	+FRT		−FRT	
	βGAL^+	βGAL^-	βGAL^+	βGAL^-
Exp 1	30	46	23	0
Exp 2	24	58	32	0

FLP-mediated recombination of marker genes has the potential to provide the basis for new forms of lineage analysis in a variety of organisms. An initial step in this direction was described in a recent report: heat shock–induced expression of FLP was used to excise, and thereby inactivate expression of, a transfected pigmentation marker in order to delineate retinal clones in *Drosophila* (*11*). The utility of such loss-of-function marking paradigms, however, is limited to tissues and organisms for which both a positive genetic marker and a negative genetic background are available. The approach additionally requires that the marker gene be present in a single copy so that individual recombination events reverse cellular phenotype. These conditions are only exceptionally met in *Drosophila* and would be more rarely met in mice. In contrast, the gain of function β-galactosidase marking system described here could be used for lineage analyses in a wide variety of tissues in different organisms. The reporter was normally silent, spontaneously activated at very low frequencies, and was efficiently activated by FLP. The gain of function was heritable and easily detected with a simple histochemical assay. In transgenic mice, the lineages marked by recombination would be determined by the promoters used to drive FLP expression. These could include promoters that were only transiently active at a developmental state that substantially preceded overt differentiation. Because transcription of the β-galactosidase construct would be controlled by an independent set of cis-acting sequences, recombined reporter genes could be expressed at later developmental stages, after differentiation had occurred. By this means it would be possible to construct a fate map for mammalian development that correlated embryonic patterns of gene expression with the organization of mature tissues.

REFERENCES AND NOTES

1. J. R. Broach and J. B. Hicks, *Cell* **21**, 501 (1980).
2. The oligonucleotide used for the construction of pFRTβGAL was 5′-GATCCCGGGCTACC**ATG**-GA·GAAGTTCCTATTC·CGAAGTTCCTATTC-(TCTAGA)AAGTATAGGAACTTCA-3′. This contained an in-frame start codon (bold), minimal FRT site (underlined), and an additional copy of the 13-bp FRT repeat (between center dots); the Xba I site within the FRT spacer is enclosed in parentheses. The linker was inserted between the Bam HI and Hind III sites of pSKS105 [M. J. Casadaban, A. Martin-Arias, S. K. Shapira, J. Chou, *Methods Enzymol.* **100**, 293 (1983)] and the *lacZ* portion of the modified gene was cloned into a pSV2 vector (*17*). The neomycin cassette used for construction of pNEOβGAL was an Xho I–Bam HI fragment from pMC1neo-polyA (*27*) cloned between copies of the J3 FRT site (*4*) in pUC19.
3. R. M. Gronostajski and P. D. Sadowski, *J. Biol. Chem.* **260**, 12320 (1985); J. F. Senecoff, R. C. Bruckner, M. M. Cox, *Proc. Natl. Acad. Sci. U.S.A.* **82**, 7270 (1985).
4. M. Jayaram, *Proc. Natl. Acad. Sci. U.S.A.* **82**, 5875 (1985).

5. S. O'Gorman and G. M. Wahl, unpublished observations.
6. pOG44 consisted of the cytomegalovirus immediate-early promoter from pCDM8 (*18*), a 5′ leader sequence and synthetic intron from pMLSIScat (*13*), the FLP coding sequence [nucleotides 5568 to 6318 and 1 to 626 of the 2-μm circle (*15*)], and the SV40 late region polyadenylation signal from pMLSIScat (*13*). The following silent nucleotide substitutions were introduced into the structural FLP sequences with the use of the polymerase chain reaction: C for T at position 5791 (*15*), G for A at 5794, G for C at 5800, C for T at 55, G for A at 58, and C for T at 55, G for A at 58, and C for T at 103. These changes eliminated three canonical AATAAA polyadenylation signals and introduced a Pst I restriction site without altering the amino acids encoded by the sequence. These alterations did not appear to significantly affect the expression of FLP by mammalian cells. pOG28 consisted of a murine cDNA for dihydrofolate reductase (*6*) cloned into pCDM8.
7. R. J. Bollag, A. S. Waldman, R. M. Liskay, *Annu. Rev. Genet.* **23**, 199 (1989).
8. pOG45 consisted of the neomycin resistance cassette and 3′ FRT from pNEOβGAL cloned into pUC19. pOG45A was derived from pOG45 by deleting a 200-bp fragment containing the FRT.
9. J. F. Senecoff, P. J. Rossmeissl, M. M. Cox, *J. Mol. Biol.* **201**, 405 (1988).
10. B. Sauer and N. Henderson, *New Biologist* **2**, 441 (1990).
11. K. G. Golic and S. Lindquist, *Cell* **59**, 499 (1989).
12. B. Sauer and N. Henderson, *Nucleic Acids Res.* **17**, 147 (1989).
13. M. T. F. Huang and C. M. Gorman, *ibid.* **18**, 937 (1990).
14. S. M. Mount, *ibid.* **10**, 459 (1982).
15. J. L. Hartley and J. E. Donelson, *Nature* **286**, 860 (1980).
16. M. T. F. Huang and C. M. Gorman, *Mol. Cell. Biol.* **10**, 1805 (1990).
17. P. J. Southern and P. Berg, *J. Mol. Appl. Genet.* **1**, 327 (1982).
18. A. Aruffo and B. Seed, *Proc. Natl. Acad. Sci. U.S.A.* **84**, 8573 (1987).
19. U. Bond, *EMBO J. 7*, 3509 (1988).
20. H. J. Yost and S. Lindquist, *Cell* **45**, 185 (1986).
21. B. Hirt, *J. Mol. Biol.* **26**, 365 (1967).
22. F. L. Graham, J. Smiley, W. C. Russel, R. Nairn, *J. Gen. Virol.* **36**, 59 (1977).
23. F. L. Graham and A. J. van der Eb, *Virology* **52**, 456 (1973).
24. J. de Wet, K. V. Wood, M. DeLuca, D. R. Helenski, S. Subramani, *Mol. Cell. Biol. 7*, 725 (1987).
25. C. V. Hall, P. E. Jacob, G. M. Ringold, F. Lee, *J. Mol. Appl. Genet.* **2**, 101 (1983).
26. J. R. Sanes, J. L. R. Rubenstein, J.-F. Nicolas, *EMBO J.* **5**, 3133 (1986).
27. K. Thomas and M. Capecchi, *Cell* **51**, 503 (1987).
28. We thank M. McKeown, R. Heyman, and R. Evans for their insightful contributions to this work and the preparation of the manuscript. M. Jayaram provided the FRT and FLP coding sequences. Supported by Xerox Corporation, Bayer A. G., the Weingart Foundation, and the Mathers Foundation.

28 August 1990; accepted 8 January 1991

Multiple Representations of Pain in Human Cerebral Cortex

JEANNE D. TALBOT, SEAN MARRETT, ALAN C. EVANS, ERNST MEYER, M. CATHERINE BUSHNELL, GARY H. DUNCAN*

The representation of pain in the cerebral cortex is less well understood than that of any other sensory system. However, with the use of magnetic resonance imaging and positron emission tomography in humans, it has now been demonstrated that painful heat causes significant activation of the contralateral anterior cingulate, secondary somatosensory, and primary somatosensory cortices. This contrasts with the predominant activation of primary somatosensory cortex caused by vibrotactile stimuli in similar experiments. Furthermore, the unilateral cingulate activation indicates that this forebrain area, thought to regulate emotions, contains an unexpectedly specific representation of pain.

DESPITE THE POWERFUL NATURE OF pain as a sensation, there is little consensus regarding the involvement of the cerebral cortex in pain processing. Early this century, Head and Holmes (*1*) observed individuals with war injuries and concluded that the cerebral cortex played only a minimal role in pain perception. Penfield and Boldrey (*2*) reached a similar conclusion when they found that patients rarely reported a sensation of pain on electrical stimulation of their exposed cerebral cortex during surgery to remove epileptic seizure foci. Thus, a commonly held view in clinical neurology is that "stimulation of . . . any . . . cortical areas in a normal, alert human being does not produce pain" (*3*).

Other data indicate that several areas of the cerebral cortex may process nociceptive information. Some patients with epileptic foci involving the primary or secondary somatosensory areas of the parietal lobe (SI and SII, respectively) experience pain during seizures (*4*). In addition, lesions of these areas in humans can sometimes lead to reduced pain perception (*5*). Single neurons in both SI and SII of the parietal cortex of awake monkey respond to nociceptive stimuli (*6*); however, these findings are so rare that the functional significance of parietal nociceptors is still in question.

Frontal cortex has also been implicated in pain processing. In cat and in humans, noxious electrical stimuli induce an increase in cerebral blood flow to the frontal lobes (*7*). In rat there are neurons in the prefrontal cortex that respond to noxious skin stimulation (*8*). In addition, in patients resection of the anterior cingulate cortex can reduce the distress associated with chronic intractable pain (*9*). Nevertheless, the unreliable nature of this surgical procedure in relieving pain (*10*) and the absence of precise anatomical data from humans, uncompromised by disease or lesions, underscore our lack of knowledge concerning the normal function of specific cortical regions in pain processing.

We have now investigated the involvement of specific cortical areas in the perception of pain in awake, healthy, human volunteers. To functionally isolate the perception of pain from all other sensory and behavioral variables, we used subtractive positron emission tomography (PET). This technique can identify subtle differences in the activation of specific brain sites relative to sensory and evaluative processes (*11, 12*). In addition, we have applied methods (*13, 14*) that combine into stereotaxic images the functional information derived

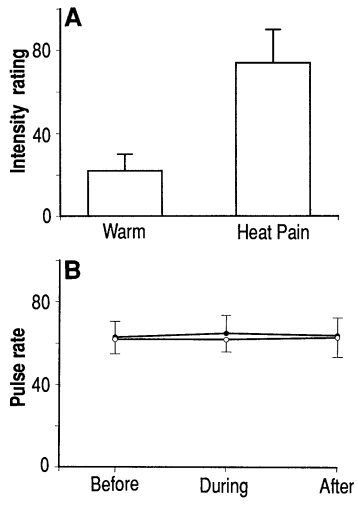

Fig. 1. (**A**) The perceived intensity of the thermal stimuli. Intensity ratings (mean ± SD) given by the eight subjects immediately after the PET scans in which the thermal stimuli were 41° to 42°C (Warm) or 47° to 49°C (Heat Pain). The ratings were different between the two conditions (paired *t* test, $t = 12.7$, $P < 0.0001$). (**B**) Mean pulse rate (±SD) of the eight subjects during 2-min epochs before, during, and after the termination of the PET scans during the Warm (○) and Heat Pain (●) conditions. A repeated-measures multivariate analysis of variance revealed no significant changes in pulse rate over time [$F(2) = 0.05$, $P = 0.95$] nor between the Warm and Heat Pain conditions [$F(1) = 0.73$, $P = 0.38$].

J. D. Talbot, M. C. Bushnell, G. H. Duncan, Laboratoire de neurophysiologie comportementale, Faculté de médecine dentaire, Université de Montréal, Montreal, Quebec, Canada H3C 3J7.
S. Marrett, A. C. Evans, E. Meyer, Positron Imaging Laboratories, McConnell Brain Imaging Center, Montreal Neurological Institute, Montreal, Quebec, Canada H3A 2B4.

*To whom correspondence should be addressed.